Journal of Power Sources 195 (2010) 5902–5908

Contents lists available at ScienceDirect

Journal of Power Sources

journal homepage: www.elsevier.com/locate/jpowsour

Fabrication of nanostructured titania on flexible substrate by electrochemical anodization

Hiroshi Nanjo*, Fathy M.B. Hassan, Shanmugam Venkatachalam, Nobuhiko Teshima, Kazunori Kawasaki, Takafumi Aizawa, Tsutomu Aida, Takeo Ebina

National Institute of Advanced Industrial Science and Technology (AIST), RC-CCP, Nigatake 4-2-1, Miyagino-ku, Sendai 983-8551, Japan

ARTICLE INFO

Article history:
Received 16 September 2009
Received in revised form
24 November 2009
Accepted 24 November 2009
Available online 3 December 2009

Keywords:
Titania nanostructure
Flexible
Electrochemical
Anodization
Heat resistance
Transparency

ABSTRACT

Titanium films were deposited on ITO (indium tin oxide)-coated PEN (polyethylene naphthalate) and flexible clay substrates by ion beam sputter deposition method. The surface morphology of the deposited films was smooth on PEN and rough on clay substrates. The titanium film deposited on Clay-mo (98% montmorillonite) substrate was anodized in ethylene glycol + 2 vol% H_2O + 0.3 wt% NH_4F solution, and the titanium films deposited on Clay-st (99% stevensite) substrate was anodized in 2-propanol + 16 vol% H_2O + 0.14 M NH_4F solution. Then nanohole-structured titania (TiO_2) films were firstly and successfully fabricated on the flexible transparent clay substrates. The nanohole structures of TiO_2 on both clay substrates were similar to those on PEN and glass substrates. The TiO_2 nanohole structure was almost maintained after annealing at 450 °C for 4 h in air. The optical transmittance of the nanohole-structured TiO_2 films on Clay-st increased from 26% to 54% at 800 nm in wavelength after annealing at 450 °C for 1 h in air.

1. Introduction

Nanostructured titania is a very attractive material due to its large surface area and thereby high electrochemical catalytic activity. Nanostructured titania was prepared in the form of several morphologies for examples, nanoparticle [1], nanorod [2], nanowire [3], nanohole [4] and nanotube [5], which can be fabricated by sol–gel method [6], hydrothermal synthesis in an alkaline solution [7] and electrochemical anodization in a solution containing fluoride ion [8], chorine ion [9] and so on. Those nanostructures are expected to be applied for photocatalytic surfaces [10], a photoanode and a cathode in a photoelectrochemical system designed to split water into hydrogen (for use in fuel cells) [11] and electrochemical electrodes such as a non-platinum cathode material of polymer electrolyte fuel cells and direct methanol fuel cells (DMFCs) [12], hydrogen sensors [13], redox capacitors [14] and dye-sensitized solar cells [15]. Among them, we focused on titania nanotube or its related structure by anodization. The nanotube-related structure can be fabricated on the bulky substrate; therefore an electron produced at the surface of nanotube can be directly transported into a current collector without large point contact resistance which occurred at the boundary between nanoparticles. Since the nanotube formed by electrochemical anodization makes array structure perpendicular to the substrate and is difficult to separate from the substrate, the recent concerns related to health risks because of the usage of nanometer size materials are less.

For energy applications, flexibility [16,17] is an important feature because it leads to low cost roll-to-roll production [18]. In addition, the wide surface area usage on not only the flat plates but also the flexible or curved surfaces, the light weight, and toughness for impact attack are highly demanded advantages for mobile applications. However, a lot of plastics are generally weak to withstand heating over 200 °C. Though titanium foils or thin plates [18–20] have flexibility and heat resistance, it is impossible to get transparency. Therefore it is necessary to find transparent, flexible and heat resistant substrate that can withstand over 300 °C in order to sinter and crystallize amorphous titania into crystalline structure such as anatase, which allows fast electron transportation and increase the quantum efficiency in several applications [12–15]. Recently we developed self-standing clay films [21,22] with flexibility, light weight and high temperature heat resistance over 450 °C. Some kinds of the clay films [23–25] have enough transparency, which is suitable for solar cells. However, so far, nanostructured titania has not been fabricated on such excellent clay films yet.

In this paper, titanium (Ti) films were deposited on clay substrates by ion beam sputter deposition method and were electrochemically anodized in fluoride-containing solutions, and then

* Corresponding author. Tel.: +81 70 6953 8414; fax: +81 22 237 7027.
E-mail address: hi-nanjo@aist.go.jp (H. Nanjo).

0378-7753/$ – see front matter © 2009 Elsevier B.V. All rights reserved.
doi:10.1016/j.jpowsour.2009.11.097

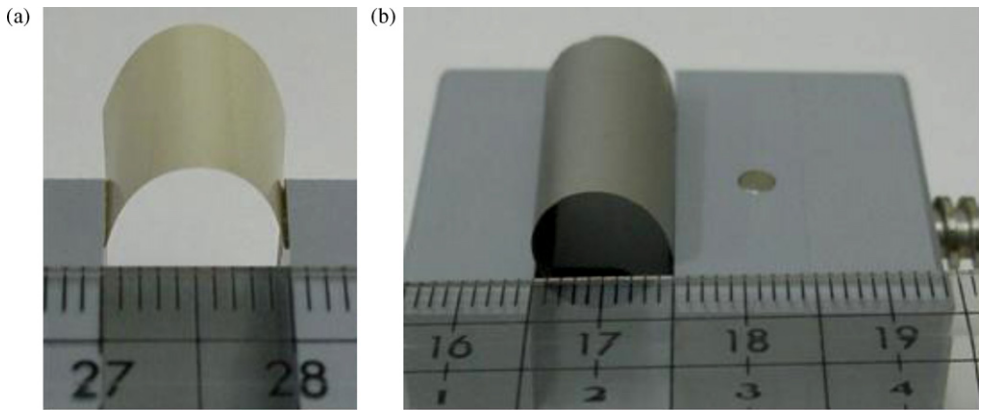

Fig. 1. Flexibility of Clay-mo with ITO film (a) and Clay-st with ITO and Ti films (b).

nanostructured titania (TiO_2) was fabricated. The surface morphology, surface roughness, structural and optical properties of the synthesized films were evaluated, and compared with the titania films which were formed on Clay-mo, polyethylene naphthalate (PEN), titanium foil, bulk titanium plate, glass and Clay-st substrate from the point of view of nanostructure, flexibility, heat resistance, transparency and so on.

2. Experimental

The Ti films were deposited by ion beam sputter deposition method (EIS-220ER, Elionix Co., Ltd.). Pure titanium (99.98% Ti) was used as a target; prior to deposition, the chamber was evacuated to a base pressure of 1×10^{-4} Pa by a turbine pump and then high purity argon gas was introduced into the chamber. Pure Ti films were deposited on flexible clay substrates coated with indium tin oxide (ITO), ITO-coated PEN and FTO (fluorine-doped tin oxide)-coated glass substrate. The thickness of the deposited Ti was about 500 nm or 290 nm while the thickness of ITO layer was 130 nm. ITO-coated PEN and FTO-coated glass with a standard electrical resistance for dye-sensitized solar cells were taken from Peccell Technology Inc. and Hohsen Corp., respectively. For comparison, Ti foil (99.5%) of 50 μm in thickness was used with the condition of as-received from Nilaco Corp. Ti plate (99.5%) of 0.5 mm in thickness was used after mechanically polishing with 9 μm diamond paste. Two kinds of clay substrates were used. The one is Clay-mo (98% montmorillonite, $X_{0.3}(Al,Mg)_2Si_4O_{10}(OH)_2{\cdot}nH_2O$, X: Li or Na) and another is Clay-st (99% stevensite, $X_{0.3}Mg_3Si_4O_{10}(OH)_2{\cdot}nH_2O$, X: Li or Na). Those were prepared by aqueous dispersion, degassing from the aqueous solution, casting in a tray and drying the solution. The precise method of clay film preparation was described in the literatures [21,22].

The anodization was performed in a solution of ethylene glycol (EG) + 2 vol% H_2O + 0.3 wt% NH_4F for Clay-mo and 2-propanol + 16 vol% H_2O + 0.14 M NH_4F for Clay-st by using Potentiostat/Galvanostat (HA-3001A, Hokuto Denko Co., Ltd.). We used two electrodes anodization system, one of which was a platinum counter electrode and another was a sample (working electrode). All the samples were anodized for an hour at an applied voltage of 20 V which was ramped from 0 to 20 V with the rate of 200 mV s^{-1} [8] for Clay-mo and 200 V s^{-1} for Clay-st. Anodized clay film was annealed at 450 °C for 4 h for Clay-mo or 1 h for Clay-st in air. The surface morphologies of the Ti films before and after anodization were observed by using field emission scanning electron microscopy (FESEM, S-4800, Hitachi High-Technologies Corp.). The structural and optical analyses of the anodized and annealed titania films were studied by X-ray diffractometer (XRD, RINT 2200VK/PC, Rigaku Corp.) and UV-VIS-NIR spectrophotometer (UV-3150, Shimadzu Corp.) or spectroscopic ellipsometry (FE-5000, Otsuka Electronics Co., Ltd.), respectively. Electrical resistance of a substrate was measured by a digital multimeter with two needles separated from each other by 1 cm. The electrical resistances

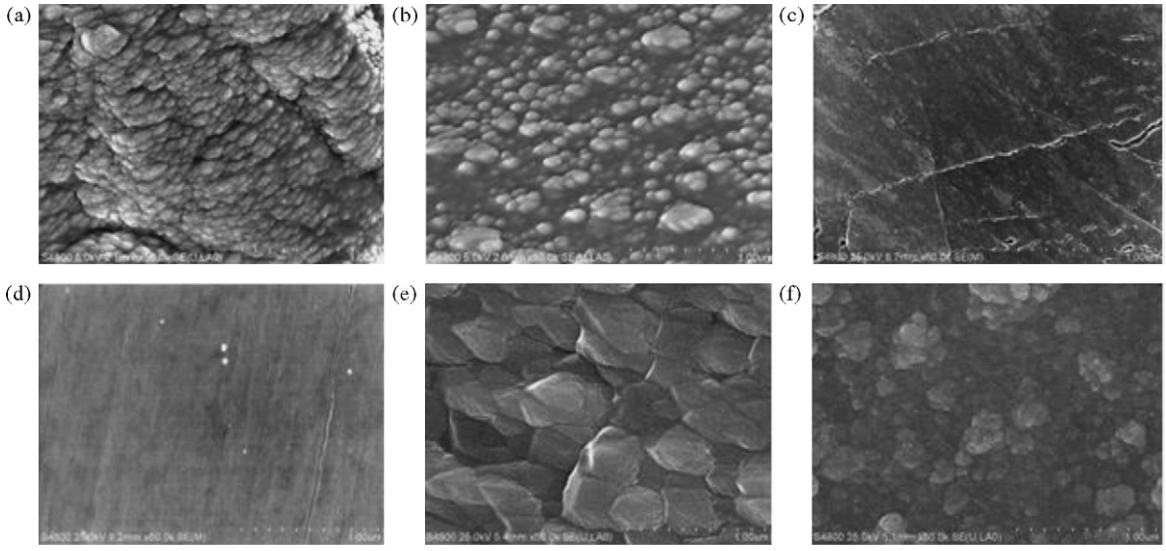

Fig. 2. SEM images of Ti surfaces before anodization; Ti/ITO/Clay-mo (a), Ti/ITO/PEN (b), Ti foil (c), bulk Ti plate (d), Ti/FTO/glass (e), and Ti/ITO/Clay-st (f).

Table 1
The properties of substrates and anodization conditions.

	Clay-mo	PEN	Foil Ti	Bulk Ti	Glass	Clay-st
Heat resistance (°C)	700	160	1668	1668	720	700
Flexibility	Good	Good	Good	Bad	Bad	Good
Transparency with TCO (%)	12.2	86.2	0	0	81.6	76.0
Sample thickness (μm)	96	207	51	502	1128	13
Ti thickness (μm)	0.5	0.5	51	502	0.5	0.29
RMS roughness (nm)[a]	105	10.1	30.8	9.23	36.8	49.8
Electrical resistance (Ω)	140	27	<0.1	<0.1	23	76
Anodization conditions	A	A	A	A	A	B

Clay-mo: 98% montmorillonite purity of (98%), Clay-st: 99% stevensite, TCO: transparent conductive oxide films of ITO or FTO, A: ramping rate of 200 mV s^{-1} and 20 V for 1 h in ethylene glycol + 2 vol% H_2O + 0.3 wt% NH_4F, B: ramping rate of 200 V s^{-1} and 20 V for 1 h in 2-propanol + 16 vol% H_2O + 0.14 M NH_4F.

[a] Surface roughness of Ti in the area of 5 μm^2 measured by atomic force microscope.

of transparent conductive oxide (TCO) films on clay substrate were larger than those on PEN and glass substrates due to the thin ITO films (130 nm) on the substrates with large surface roughness.

The important properties of the substrates and anodization conditions were summarized in Table 1.

3. Results and discussion

3.1. Characterization of the substrate materials

Fig. 1 shows the flexibility of the Clay-mo with ITO film and Clay-st with ITO and Ti films. It was found that ITO-coated Clay-mo substrate had good flexibility of ca. 10 mm in curvature diameter [23–26]. It reveals that the flexibility of ITO-coated Clay-mo substrate was close to that of Ti foil and it was much better than bulk Ti plate and Ti-coated FTO/glass substrate.

Fig. 2 shows the surface morphologies of Ti films on ITO-coated Clay-mo and PEN, FTO-coated glass substrates and Ti foil and bulk Ti plate before anodization. Ti film on Clay-mo had particle-like structure with very large surface roughness; its root mean square roughness (RMS) was measured as 105 nm. The RMS roughness of Ti film on Clay-mo substrate was larger than that of other substrates. Ti on PEN also had particle-like structure with small RMS roughness of 10.1 nm. Ti foil had smooth surface and long clacks. Polished-bulk Ti plate also had a very smooth surface with an RMS roughness of 9.2 nm. Ti films on FTO-coated glass substrate had grain-like structure; it is due to the FTO grains on the substrate. The properties of Clay-st are mentioned later. It was found that Ti films had widely different morphologies on different substrates.

3.2. Electrochemical anodization

Fig. 3(a) shows the current density variation with anodization time. The current density increased with time up to initial 100 s due to ramping period of applied voltage. Under constant potential of 20 V, current density continued to go down. The current density of Clay-mo was larger than those of the other substrates, probably because of large surface roughness, that is, wide surface area. Generally rough surface is hard to be covered with strong barrier oxide film. Therefore current density was also hard to rapidly go down in comparison with the other smoother substrates. Fig. 3(b) shows the current density variation of Ti on Clay-st in 2-propanol + 16 vol% H_2O + 0.14 M NH_4F. The current density after 100 s rapidly decreased with time in comparison with Clay-mo sample, probably because of smaller roughness (49.8 nm for Clay-st <105 nm for Clay-mo) as shown in Table 1.

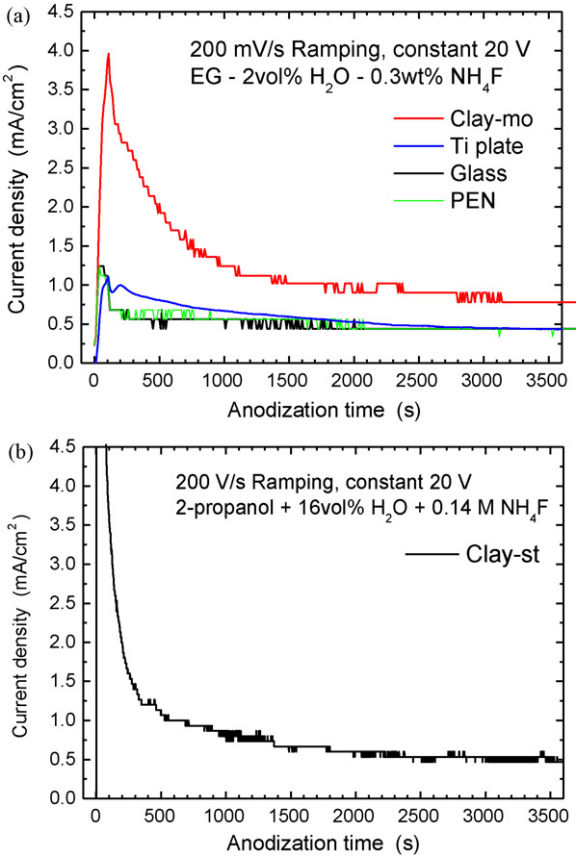

Fig. 3. Current density variation during anodization with time. (a) Ti/ITO/Clay-mo, bulk Ti plate, Ti/FTO/Glass, Ti/ITO/PEN and (b) Ti/ITO/Clay-st samples.

In the early stages of the anodization, the Ti surface is oxidized at the high potential according to the following reaction [8,27];

$$Ti_{(s)} + 2H_2O_{(l)} = TiO_{2(s)} + 4H^+ + 4e^- \quad (1)$$

Eventually, F^- ions start etching the TiO_2 surface at several sites. This reaction is called high field dissolution because it is assisted by applying the high anodization potential of 20 V;

$$TiO_2 + 4H^+ + 6F^- = TiF_6^{2-} + 2H_2O \quad (2)$$

The Reaction (1) continues leading to growth of the TiO_2 compact (barrier) layer in the direction of the film thickness. At the same time the Reaction (2) also continues leading to deeper nanoholes and the nanoporous layer grows towards the film thickness just following the compact layer. As the anodization proceeds, at the proper anodization conditions, both reactions reach equilibrium leading to that the observed current tends to reach equilibrium or steady state current value.

3.3. Morphology and composition of the anodized surfaces

Fig. 4 shows the surface morphologies of anodized-Ti films on the several kinds of substrates. The surface morphology of polished-Ti plate after anodization shows the titania nanotubes in Fig. 4(d). The intertubular distances were slightly narrow and almost all the nanotubes were in contact with each others. This anodization behavior is characteristic of the electrolytes based on ethylene glycol, 2 vol% H_2O and 0.3 wt% NH_4F in comparison with the fluoride and water solutions containing glycerol [8] or 2-propanol [28]. Anodized-Ti films did not exhibit nanotubular structures on PEN and glass substrates, but nanohole-structured titania films were formed on PEN and glass substrates (Fig. 4(b

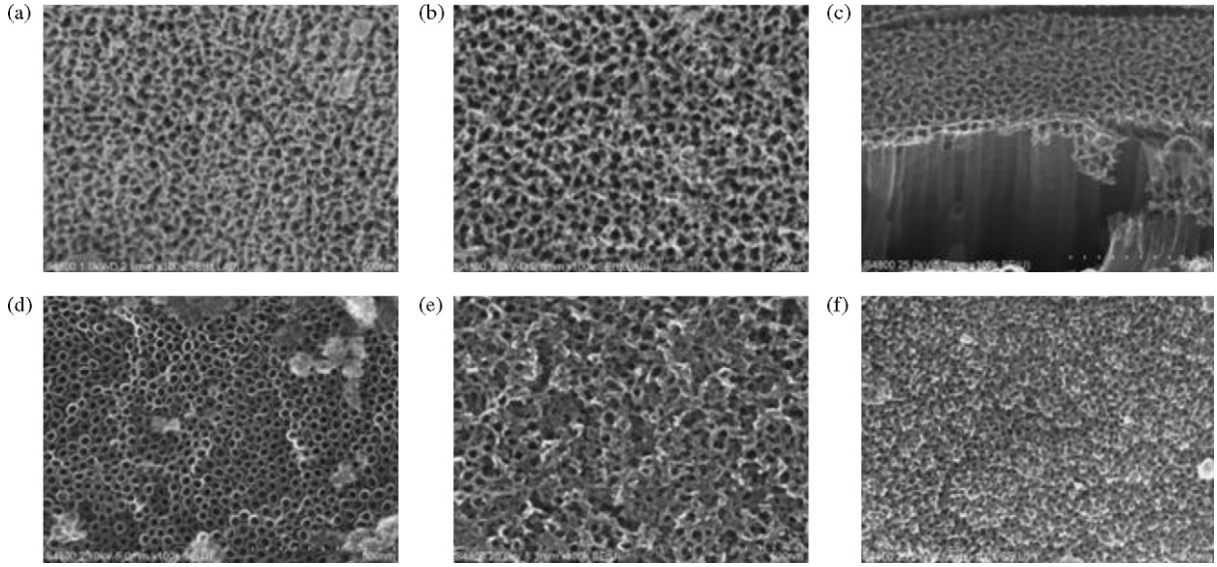

Fig. 4. SEM images of Ti surfaces after anodization; Ti/ITO/Clay-mo (a), Ti/ITO/PEN (b), Ti foil (c), bulk Ti plate (d), Ti/FTO/glass (e) and Ti/ITO/Clay-st (f).

and e)). On the other hand, though nanohole layer covered the surface, under the nanohole surface nanotubes on Ti foil were in contact with each others which are clearly shown at the right center in Fig. 4(c). The nanohole-structured titania with very huge number of density was also formed on Clay-mo substrate, which was very similar to those on PEN and glass substrates. The diameter and the interval of the nanohole were ca. 35 and 5 nm, respectively. The nanohole interval was very similar in size to the wall thickness of common nanotubes [8]. Such small interval gives wide surface area. When we suppose the bottom region of the nanotubes; though very long nanotubes are weak and it can be easily broken in the bottom region, the nanohole structure with very large number of density is strong which improves the nanotube strength in the bottom region. It was reported by Kalantar-zadeh et al. [29] that nanopores were generated on DC-sputtered Ti films at 600 °C and nanotubes were generated on RF-sputtered Ti films at 300 °C and those structures were mainly depended on the crystal planes. That is, nanopores were observed on Ti (1 0 0) or (0 0 2) planes and nanotubes were observed on Ti (1 0 1) plane. It was considered according to this paper that since the Ti films deposited by ion beam sputtering do not have (1 0 1) plane, i.e., no nanotubes but nanoholes were fabricated.

The nanohole-structured titania film on ITO-coated Clay-mo substrates (Fig. 4(a)) was then annealed at 450 °C for 4 h in air. Fig. 5 shows the surface morphologies of annealed titania films on ITO-coated Clay-mo substrates. The top of the surface became round by long time annealing and TiO_2 grains were expected to grow (Fig. 5(a)), which probably assists better electron transportation because of the reduction in number of grain boundaries. The thickness of the oxide layer shown with a white arrow was 600 nm calculated from the tilted view at 60° as shown in Fig. 5b. The cylindrical holes were confirmed at the section region around the white arrow. TiO_2 nanostructure on Clay-mo was almost maintained after annealing at 450 °C for 4 h in air. On the other hand, it was confirmed in a preliminary test that in a high vacuum condition lower than 4×10^{-5} Pa, the color of Clay-mo substrate turned from white into black after annealing at 450 °C for an hour. Therefore, annealing in air was a suitable condition which improves the optical transmittance of the clay substrate, which is appropriate for solar cell electrodes.

Fig. 6 shows X-ray diffraction patterns of nanostructured-Ti films on ITO-coated Clay-mo substrate before and after anodization. In Fig. 6, the peaks marked as "m" correspond to the Clay-mo substrate. After anodization, a few peaks in the X-ray diffraction pattern were split into two due to the swelling because clay sheets absorbed water or interacted with the electrolyte. Since Ti films deposited at room temperature and its anodized titania were both amorphous [27], diffraction peaks of Ti and titania were not observed. After annealing at 450 °C for 4 h, the separated peaks of Clay-mo were united and crystalline anatase and titania (PDF#35-0088) were detected (see Fig. 6).

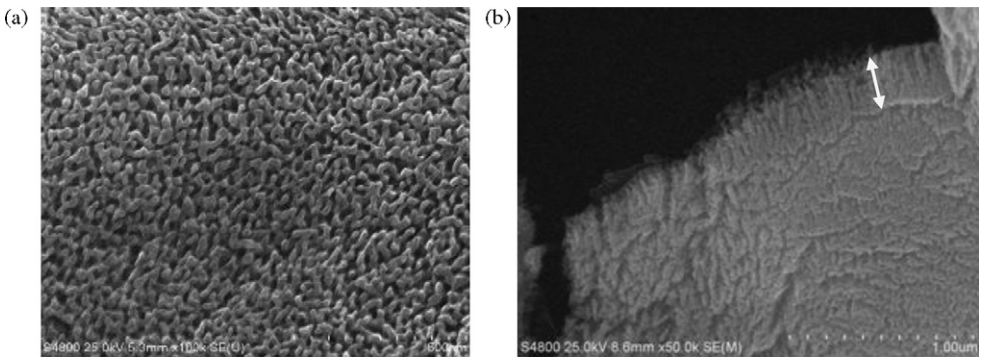

Fig. 5. SEM images of anodized and annealed Ti/ITO/Clay-mo. (a) Top view and (b) 60°-tilted view.

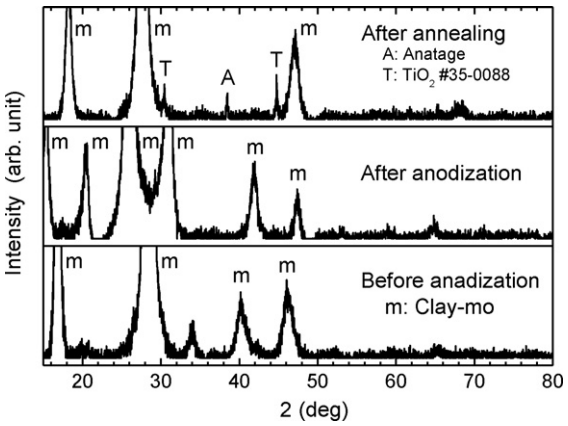

Fig. 6. X-ray diffraction patterns of Ti/ITO/Clay-mo sample before anodization, after anodization and after annealing at 450 °C for 4 h in air.

3.4. Morphology and composition of the anodized surface of Clay-st

Clay-mo gets swollen after anodization as mentioned in the previous section and it was confirmed in a test the optical transmittance of the Clay-mo substrate was measured as 12.2% at 800 nm in wavelength (figure not shown). Here, another clay film called as Clay-st was introduced. In this case, firstly Clay-st substrate was annealed at 550 °C for 24 h and then ITO films were deposited on Clay-st substrate. Interestingly this annealing process has changed the Clay-st substrate property from hydrophilic into hydrophobic, which was very convenient for electrochemical anodization because the swelling of clay substrate can be inhibited. After deposition of 130 nm ITO film, the optical transmittance was measured as 76.0% at 797 nm in wavelength (Table 1). Then Ti film of 290 nm in thickness was deposited on ITO-coated Clay-st substrate. The flexibility of Ti/ITO/Clay-st system was measured as 10 mm in diameter as shown in Fig. 1(b). The Ti/ITO/Clay-st system has smooth surface with an RMS roughness of 49.8 nm, its surface roughness was lower than that of Clay-mo substrate (RMS = 105 nm) (see Fig. 2(f)).

Fig. 4(f) shows the surface morphology of the Ti/ITO/Clay-st sample after anodization. It shows that nanohole-structured titania was formed on Clay-st substrate. Here the electrochemical anodization was performed in 2-propanol + 16 vol% H_2O + 0.14 M NH_4F for an hour. The nanohole diameter was measured as 25 nm, but the nanohole diameter on Clay-mo was measured as 35 nm (see Fig. 4(a)). It shows that the nanohole diameter of titania on Clay-st substrate is smaller than that on Clay-mo substrate. The interval between the nanoholes on Clay-st was wider than that on Clay-mo. Such a wide interval of nanostructure was seen on bulk Ti plate anodized in 2-propanol + 16 vol% H_2O + 0.14 M NH_4F [28]. Whereas, it was observed in Fig. 7(a) that the other nanohole morphology on Clay-st was almost same with that on Clay-mo. Inspection of Fig. 7(b) and (e) revealed that the nanohole morphology and X-ray diffraction pattern did not apparently change before and after annealing at 450 °C for 1 h in air. Tetsuka et al. [23] reported that a flexible and transparent clay film (saponite–20% sodium polyacrylate) was decomposed at 460 °C and was dehydroxylated at 740 °C. It was clarified that titania nanohole structure

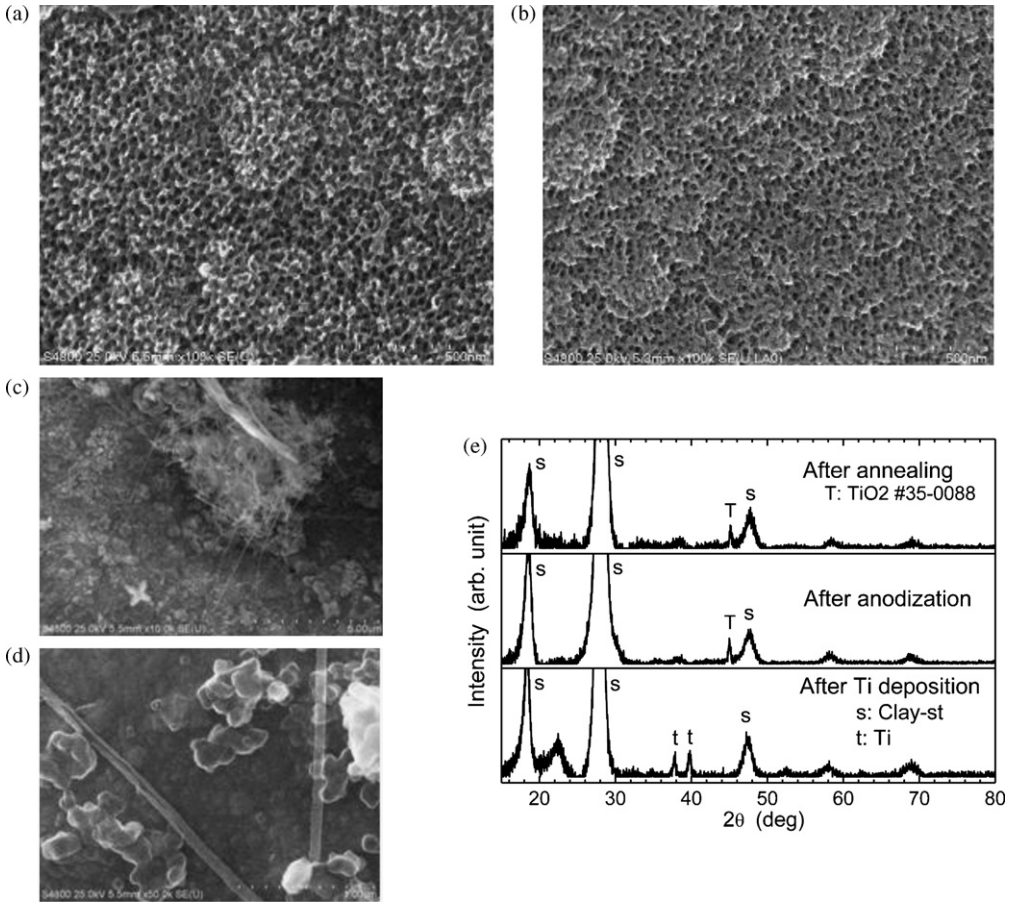

Fig. 7. SEM images and XRD patterns of Ti/ITO/Clay-st. (a) After anodization in 2-propanol–H_2O–NH_4F, (b) after annealing at 450 °C for 1 h in air, (c) and (d) titania nanotubes laying on the surface, (e) X-ray diffraction patterns Ti/ITO/Clay-st sample before anodization, after anodization and after annealing at 450 °C for 1 h in air.

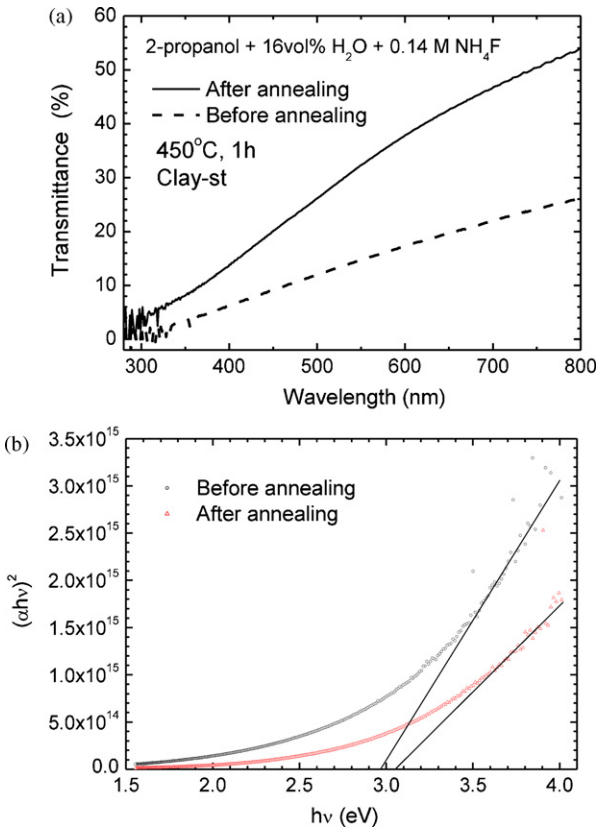

Fig. 8. Optical transmittance spectra (a) and Tauc's plot (b) of anodized nanostructured TiO_2 on Clay-st substrate before and after annealing at 450 °C for an hour in air.

has also good heat resistance over 450 °C, which allows crystallization of amorphous titania on clay substrates. In Fig. 7(e), since Ti diffraction peaks disappeared after anodization and annealing for 1 h in air, it reveals that the Ti film was almost consumed in the anodization process and converted almost entirely into titania, TiO_2. This helps to increase the optical transmittance of Clay-st sample.

On a part of the surface, an assembly of very long nanotubes over 9 μm in length with an outer diameter of 100 nm was observed (see Fig. 7(d)). It seems that broken seeds of nanotubes rapidly grew by assistance of excessive high density of $[TiF_6]^{2-}$ and their precipitation with the form of nanotube on the surface. Such type of long nanotubes lying on a bulk Ti plate was also seen in the literature [28].

3.5. Optical properties of the modified clay film

Fig. 8(a) shows the optical transmittance spectra of the nanostructured titania films on ITO-coated Clay-st substrate, which was measured by spectroscopic ellipsometer. The optical transmittance of the TiO_2 film before annealing was measured as 26% at 800 nm in wavelength. Since the optical transmittance of TiO_2/ITO/Clay-mo sample was found to be 0.2% at 800 nm, the optical transmittance of TiO_2/ITO/Clay-st sample was much higher than that of TiO_2/ITO/Clay-mo sample; it is due to low purity of Clay-mo substrate, swelling under anodization and surface scattering. The maximum optical transmittance of TiO_2/ITO/Clay-st sample increased from 26% to 54% at 800 nm after annealing at 450 °C for an hour in air. It is attributed that small amount of metallic titanium, which was not detected by X-ray diffraction, was almost entirely oxidized by annealing, and that optical scattering decreases, i.e., grain boundary decreases after annealing at 450 °C for an hour in air [30].

Based on the data of Fig. 8(a), the optical band gap of titania on ITO-coated Clay-st substrate was calculated from Tauc's plot as shown in Fig. 8(b). It reveals that the optical band gap increased from 2.97 eV before annealing to 3.08 eV after annealing. Though those values were slightly lower than 3.09 eV for as-grown TiO_2 nanotube powder and 3.13 eV for the annealed one at 480 °C in the literature [31]. However, the tendency of increasing of band gap after annealing agreed with the literature.

4. Conclusions

Pure titanium films were sputter-deposited on different clay substrates (Clay-mo and Clay-st) coated with ITO films, and the titanium films on ITO-coated Clay-mo substrates were anodized in an ethylene glycol + 2 vol% H_2O + 0.3 wt% NH_4F solution, and the titanium films on ITO-coated Clay-st substrates were anodized in 2-propanol + 16 vol% H_2O + 0.14 M NH_4F solution. Then titania (TiO_2) nanohole structure was firstly and successfully fabricated on the flexible transparent clay films. The nanohole structures of TiO_2 on both clays substrates were similar to those on PEN and glass substrate. The TiO_2 nanohole structure was almost maintained after annealing at 450 °C for 4 h in air. The optical transmittance of Clay-st increased from 26% to 54% at 800 nm in wavelength after annealing at 450 °C for an hour in air.

Acknowledgements

The authors thank Mr. K. Motegi, Tomoegawa Co., Ltd. for making ITO film on clay films. This work was supported in part by Iketani Science and Technology Foundation and a Grant-in-Aid for Scientific Research from the Ministry of Education, Culture, Sports, Science, and Technology under contract No. 21-09509.

References

[1] K.-M. Lee, V. Suryanarayanan, K.-C. Ho, J. Power Sources 188 (2009) 635.
[2] B. Liu, E.S. Aydil, J. Am. Chem. Soc. 131 (2009) 3985.
[3] X. Feng, K. Shankar, O.K. Varghese, M. Paulose, T.J. Latempa, C.A. Grimes, Nano Lett. 8 (2008) 3781.
[4] T. Hamaguchi, M. Uno, K. Kurosaki, S. Yamanaka, J. Alloys Compd. 386 (2005) 265.
[5] F.M. Bayoumi, B.G. Ateya, Electrochem. Commun. 8 (2006) 38.
[6] D. Eder, M.S. Motta, I.A. Kinloch, A.H. Windle, Physica E 37 (2007) 245.
[7] Z.-Y. Yuan, B.-L. Su, Colloid Surf. A: Physicochem. Eng. Asp. 241 (2004) 173.
[8] F.M.B. Hassan, H. Nanjo, M. Kanakubo, I. Ishikawa, M. Nishioka, J. Surf. Sci. Nanotech. 7 (2009) 84.
[9] N.K. Allam, K. Shankarb, C.A. Grimes, J. Mater. Chem. 18 (2008) 2341.
[10] J. Yu, M. Zhou, Nanotechnology 19 (2008) 045606.
[11] S. Baea, E. Shimb, J. Yoonc, H. Joo, J. Power Sources 185 (2008) 439.
[12] M. Wang, D.-J. Guo, H.-L. Li, J. Solid State Chem. 178 (2005) 1996.
[13] O.K. Varghese, D. Gong, M. Paulose, K.G. Ong, C.A. Grimes, Sens. Actuator B: Chem. 93 (2003) 338.
[14] Y. Xie, L. Zhou, C. Huang, H. Huang, J. Lu, Electrochim. Acta 53 (2008) 3643.
[15] M.S. Akhtar, J.M. Chun, O.B. Yang, Electrochem. Commun. 9 (2007) 2833.
[16] F. Pichot, J.R. Pitts, B.A. Gregg, Langmuir 16 (2000) 5626.
[17] X. Li, H. Lin, J. Li, N. Wang, C. Lin, L. Zhang, J. Photochem. Photobiol. A: Chem. 195 (2008) 247.
[18] D. Kuang, J. Brillet, P. Chen, M. Takata, S. Uchida, H. Miura, K. Sumioka, S.M. Zakeeruddin, M. Gratzel, ACS Nano. 2 (2008) 1113.
[19] K. Nakayama, T. Kubo, Y. Nishikitani, Appl. Phys. Express 1 (2008) 112301.
[20] C.-J. Lin, W.-Y. Yu, S.-H. Chiena, Appl. Phys. Lett. 93 (2008) 133107.
[21] H.J. Nam, T. Ebina, R. Ishii, H. Nanzyo, F. Mizukami, Clay Sci. 13 (2007) 159.
[22] K. Kawasaki, K. Sakakibara, F. Mizukami, T. Ebina, Clay Sci. 13 (2008) 217.
[23] H. Tetsuka, T. Ebina, H. Nanjo, F. Mizukami, J. Mater. Chem. 17 (2007) 3545.
[24] H. Tetsuka, T. Ebina, T. Tsunoda, H. Nanjo, F. Mizukami, Nanotechnology 18 (2007) 355701.
[25] H. Tetsuka, T. Ebina, T. Tsunoda, H. Nanjo, F. Mizukami, Surf. Coat. Technol. 202 (2008) 2955.
[26] H. Tetsuka, T. Ebina, T. Tsunoda, H. Nanjo, F. Mizukami, Jpn. J. Appl. Phys. 47 (2008) 1894.

[27] Y.-X. Tang, J. Tao, Y.-Y. Zhang, T. Wu, H.-J. Tao, Y.-R. Zhu, Trans. Nonferrous Met. Soc. China 19 (2009) 192.
[28] F.M.B. Hassan, H. Nanjo, H. Tetsuka, M. Kanakubo, T. Aizawa, M. Nishioka, T. Ebina, Trans 214th Int. Sym. Electrochem. Soc., vol. 16, 2009, p. 35;
F.M.B. Hassan, H. Nanjo, H. Tetsuka, M. Kanakubo, T. Aizawa, M. Nishioka, T. Ebina, J. Electrochem. Soc. 156 (2009) K227.
[29] K. Kalantar-zadeh, A.Z. Sadek, H. Zheng, J.G. Partridge, D.G. McCulloch, Y.X. Li, X.F. Yu, W. Wlodaeski, Appl. Surf. Sci. 256 (2009) 120.
[30] Y.Z. You, Y.S. Kim, D.H. Choi, H.S. Jang, J.H. Lee, D. Kim, Mater. Chem. Phys. 107 (2008) 444.
[31] N.F. Fahim, T. Sekino, Chem. Mater. 21 (2009) 1967.